8. GROUNDWATER AND TERRESTRIAL WATER STORAGE—M. Rodell and D. Wiese

Changes in terrestrial water storage (TWS), which is the sum of groundwater, soil moisture, surface water, snow, and ice, have been measured on regional to global scales by the Gravity Recovery and Climate Experiment (GRACE) and GRACE Follow On (GRACE-FO) satellite missions on a monthly basis since 2002 (Tapley et al. 2004; Landerer et al. 2020). Interannual changes tend to be dominated by snow and ice at high latitudes and in alpine regions, by surface water in the wet tropics, and by groundwater elsewhere (Getirana et al. 2017).

Plate 2.1p displays observed changes in mean annual TWS between 2021 and 2020 as equivalent heights of water in cm. Changes in TWS were mixed across Eurasia. Most of western Europe continued to recover from the 2019 drought, while Scandinavia in the north dried (lost TWS) after a wet 2020. Copious rain increased TWS in southern India, where it was already elevated at the start of the year. To the east, the Indochina peninsula recovered from drought, receiving abundant rainfall from Typhoon Surigae (see section 4g5). Northeastern China also gained water, while drought afflicted areas south and west of the Caspian Sea. In Australia, TWS increased along the northern and southeastern coasts. Droughts in Africa caused TWS decreases in Angola and Madagascar, while TWS increased rapidly in Zimbabwe and adjacent areas at the start of 2021, including a 2-m increase in the level of Lake Kariba. In North America, TWS declines extended from southern California into southern Canada, regions where drought conditions prevailed, and across to the Great Lakes region, where declines exceeded 12 cm equivalent height of water in some parts. However, TWS in the center of the continent (including the Great Lakes region) had been elevated since 2019, when record flooding occurred, and the decrease in 2021 was largely a return to more typical conditions. Northern South America gained a massive amount of water, with increases exceeding 12 cm over a large area, but TWS declined in southern Brazil.

Time series of zonal mean and global mean monthly TWS anomalies, after removing the seasonal cycle, are plotted in Figs. 2.32 and 2.33, respectively. TWS declines in Antarctica, Greenland, the Gulf Coast of Alaska, and polar islands are attributed to ice sheet and glacier ablation as opposed to meteorological variations, so those regions were excluded from the calculations for Figs. 2.32 and 2.33. However, the effects of additional high latitude ice mass losses remain. The large TWS increase, seen straddling the equator in Fig. 2.32, corresponds to the massive wet anomaly in northern South America. The TWS decline just south of 30°N is due almost entirely to long-term groundwater depletion in northern India (Rodell et al. 2018), exacerbated by a drought just east of that area in 2021 (section 2d10). The TWS decline near 40°N mainly reflects drought across the western and central United States, drought stretching from Turkey to the Caspian Sea (including water level declines in that sea), and long-term groundwater depletion associated with agricultural irrigation in the North China Plain (Rodell et al. 2018). Droughts in southern Brazil and Angola caused the TWS decline near 15°S. Overall, global-scale TWS variability in 2021 was muted compared with past years (Plate 2.1p). Owing to the scarcity of in situ TWS measurement records, we relied on TWS data derived from GRACE and GRACE-FO satellite observations of Earth's time-varying gravity field. Uncertainty in the derived TWS anomalies is heterogeneous, but as a point of reference, uncertainty in monthly TWS anomalies is typically around 1–2 cm equivalent height of water at 500,000 km2 and larger scales (Wiese et al. 2016).

References

Getirana, A., S. Kumar, M. Girotto, and M. Rodell (2017), Rivers and floodplains as key components of global terrestrial water storage variability, *Geophys. Res. Lett.,* **44** (20), 10,359-10,368, doi:10.1002/2017GL074684.

Landerer, F.W., F.M. Flechtner, H. Save, F.H. Webb, T. Bandikova, W.I. Bertiger, S.V. Bettadpur, S.H. Byun, C. Dahle, H. Dobslaw, and E. Fahnestock (2020), Extending the global mass change data record: GRACE Follow-On instrument and science data performance. *Geophys. Res. Lett.*, **47** (12), doi:10.1002/2020GL088306.

Rodell, M., J.S. Famiglietti, D.N. Wiese, J.T. Reager, H.K. Beaudoing, F.W. Landerer (2018), and M.-H. Lo, Emerging trends in global freshwater availability, *Nature,* 557, 651-659, doi:10.1038/s41586-018-0123-1.

Tapley, B. D., S. Bettadpur, J. C. Ries, P. F. Thompson, and M. M. Watkins (2004), GRACE measurements of mass variability in the Earth system, *Science*, **305**, 503-505.

Wiese, D.N., F.W. Landerer, and M.M. Watkins (2016), Quantifying and reducing leakage errors in the JPL RL05M GRACE mascon solution. *Water Resour. Res.*, **52**, 7490-7502.

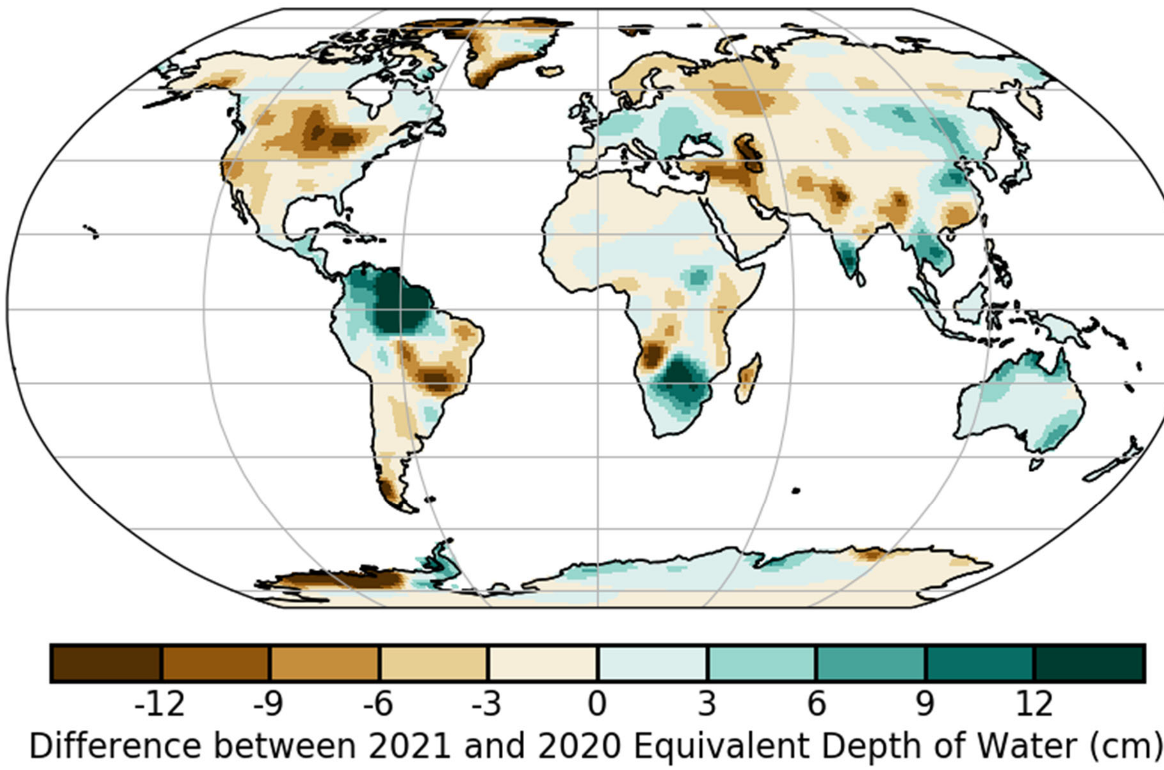

Figure 1. Changes in annual-mean terrestrial water storage (the sum of groundwater, soil water, surface water, snow, and ice, as an equivalent height of water in cm) between 2020 and 2021, based on gravity observations from the GRACE and GRACE-FO satellite missions.

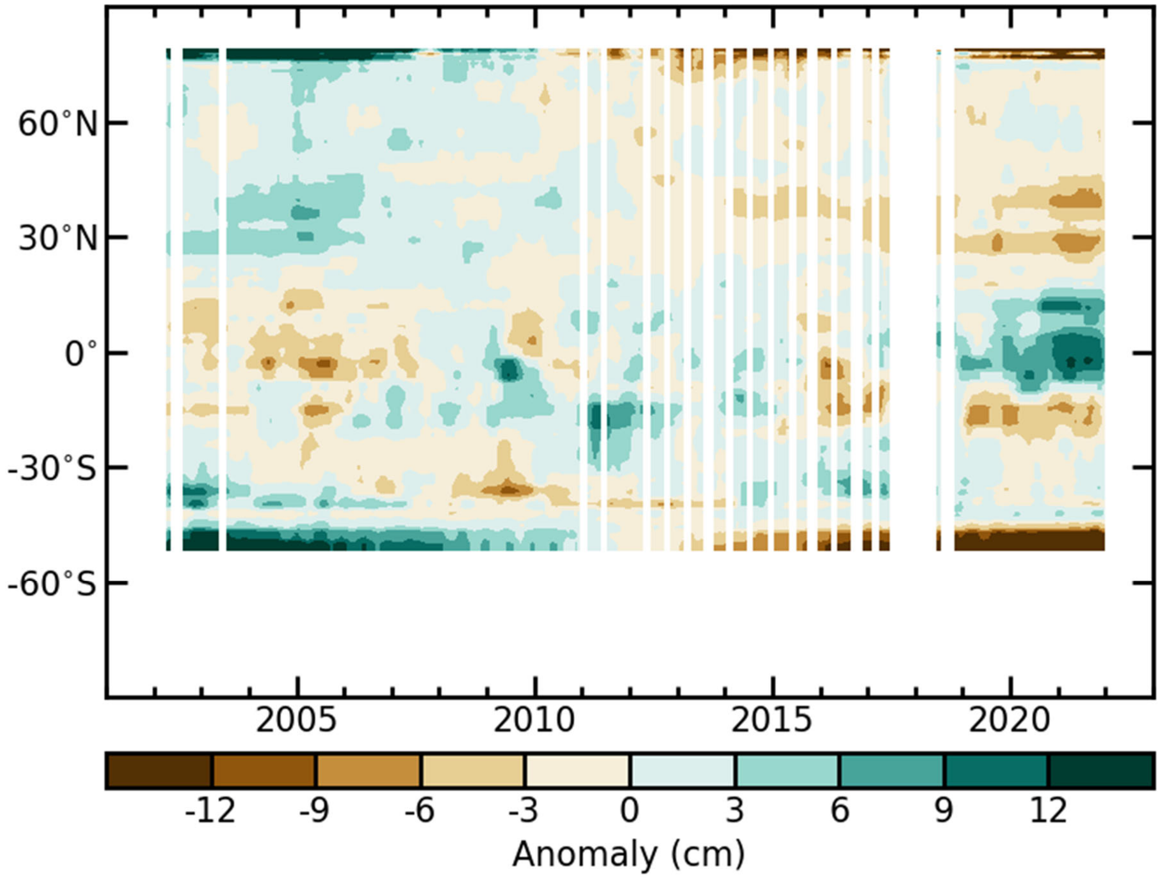

Figure 2. Zonal means of terrestrial water storage anomalies, excluding those in Antarctica, Greenland, the gulf coast of Alaska, and polar islands, in cm equivalent height of water, based on gravity observations from GRACE and GRACE-FO. The anomalies are relative to a base period of 2003-2020.

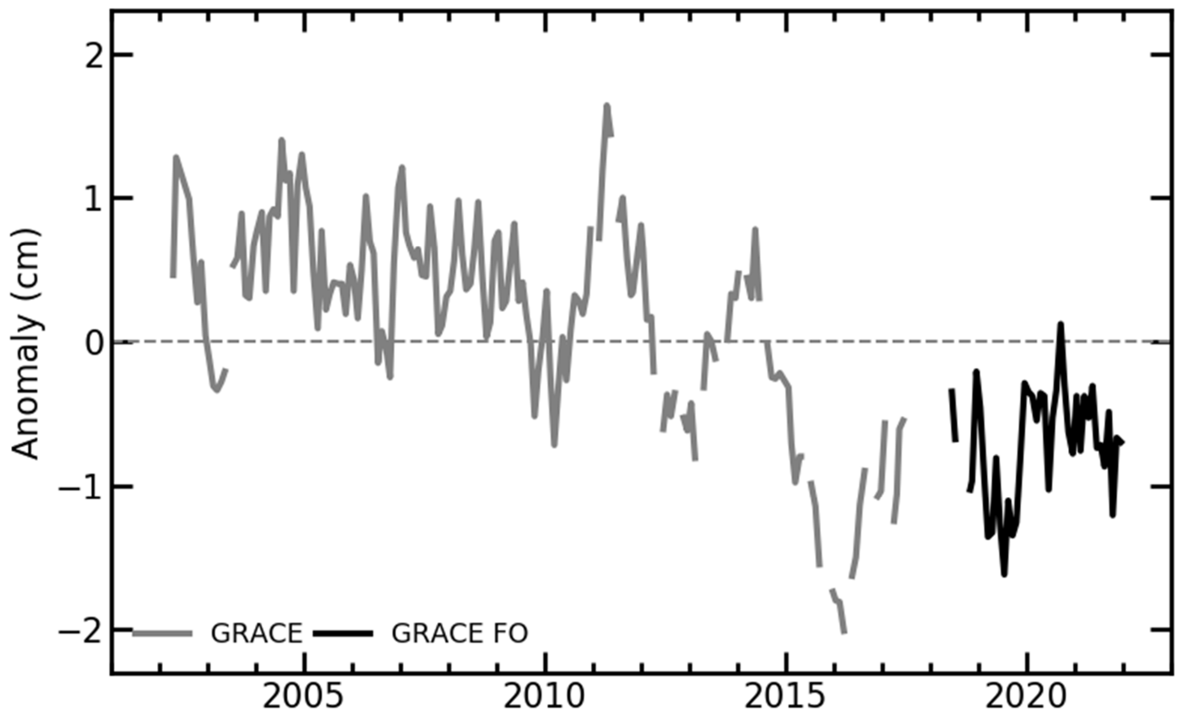

Figure 3. Global average terrestrial water storage anomalies from GRACE (gray) and GRACE-FO (black), in cm equivalent height of water, relative to a 2003-2020 mean baseline.

Datasets used and their URLs

JPL GRACE Mascon Ocean, Ice, and Hydrology Equivalent Water Height RL06 CRI Filtered Version 02. https://podaac.jpl.nasa.gov/dataset/TELLUS_GRAC-GRFO_MASCON_CRI_GRID_RL06_V2

Water Level Time Series (Altimetry) for Lake Kariba, from the Database for Hydrological Time Series of Inland Waters (DAHITI), Deutsches Geodätisches Forschungsinstitut, Technische Universität München. https://dahiti.dgfi.tum.de/en/31/time_series/

Acknowledgements

N/A